The energy gap at the first zone boundary $(k = \pi/a)$ is therefore $|d_1|$, and quite generally the energy gap at the jth zone boundary is $|d_j|$.

This result can be readily obtained by diagonalizing the degenerate two-dimensional submatrix of the Hamiltonian matrix (27) appropriate at the jth zone boundary, i.e.

$$\begin{bmatrix} \dfrac{\pi^2 j^2}{a^2} + \dfrac{d_0}{2} & \dfrac{d_j}{2} \\[2ex] \dfrac{d_j}{2} & \dfrac{\pi^2 j^2}{a^2} + \dfrac{d_0}{2} \end{bmatrix}$$

Hence

$$E(k = \pi j/a) = \frac{\pi^2 j^2}{a^2} + \frac{d_0}{2} \pm \frac{d_j}{2}. \tag{53}$$
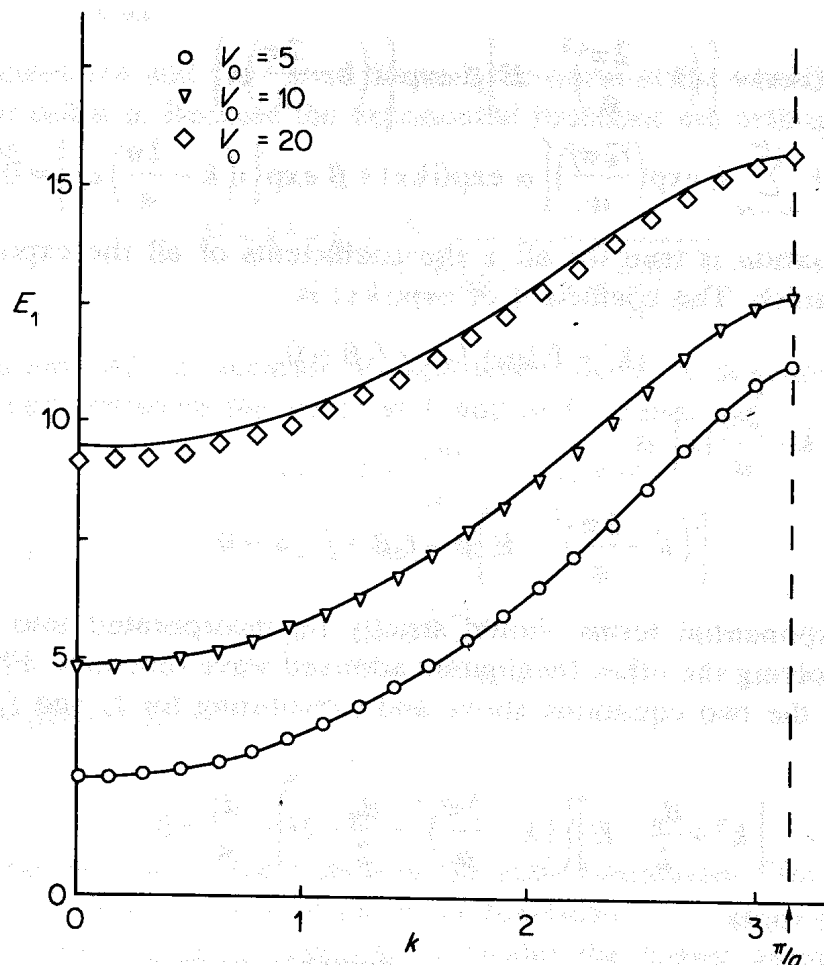

Figure 6. The results for the $E–k$ relationship of the lowest band found by the computer program with a sawtooth potential of period 1.0 for $V_0 = 5(\bigcirc)$, $V_0 = 10(\nabla)$ and $V_0 = 20(\Diamond)$. The solid curves show the predictions of the nearly-free electron approximation

Figure 6 shows a comparison between the results of the computer program (the data points) and the nearly-free electron approximation (the solid curves) for the $E-k$ relationship of the lowest band for three values of V_0 with the sawtooth potential. In this case agreement deteriorates for *high* V_0. Figure 7 shows the results of a series of program runs for the energy gap at the first zone boundary (the circles) as a function of V_0, for the sawtooth potential. The solid line shows the prediction of the nearly-free electron approximation, i.e. $4V_0/\pi^2$. Agreement decreases at large V_0.

It is of some interest to determine the coefficients α and β, and hence the wave function, especially at the zone boundary. Now using equations (23) and (49)

$$\alpha\left(k^2+\frac{d_0}{2}-E\right) = -\beta\frac{d_1}{2}, \tag{54}$$

and, at the zone boundary.
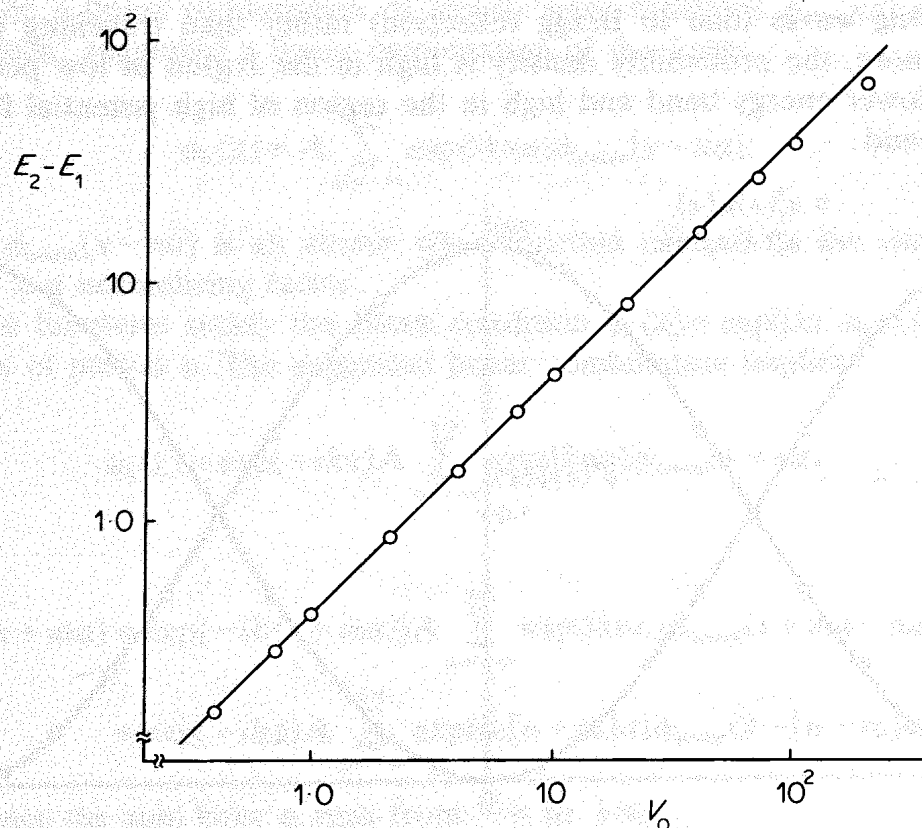
$$E = k^2+\frac{d_0}{2}\pm\frac{d_1}{2}. \tag{55}$$

Figure 7. The energy gap at the first zone boundary: $E_2(k = \pi/a)-E_1(k=\pi/a)$ as a function of V_0. The circles show the results of the computer program for a sawtooth potential of period 1.0. The solid line shows the prediction of the nearly-free electron approximation

If $d_1 < 0$, which is the case here for $V_0 > 0$, then for the lowest energy band the upper sign in equation (55) is taken and

$$\alpha\left(-\frac{d_1}{2}\right) = -\beta\left(\frac{d_1}{2}\right). \tag{56}$$

The normalization requires $\alpha^2 + \beta^2 = 1$ so that for the lowest band, at the zone boundary,

$$\psi(x) = \frac{1}{\sqrt{2}}\left[\exp\left(\frac{i\pi x}{a}\right) + \exp\left(-\frac{i\pi x}{a}\right)\right]$$

$$= \sqrt{2}\cos\left(\frac{\pi x}{a}\right). \tag{57}$$

For the second band at $k = \pi/a$, a similar analysis gives

$$\psi(x) = i\sqrt{2}\sin\left(\frac{\pi x}{a}\right). \tag{58}$$

Thus, for both bands, the wave functions at the zone boundary correspond to standing waves (due to Bragg reflection) rather than travelling waves. Furthermore, the probability density is high in the region of low potential for the lower energy band and high in the region of high potential for the higher band.
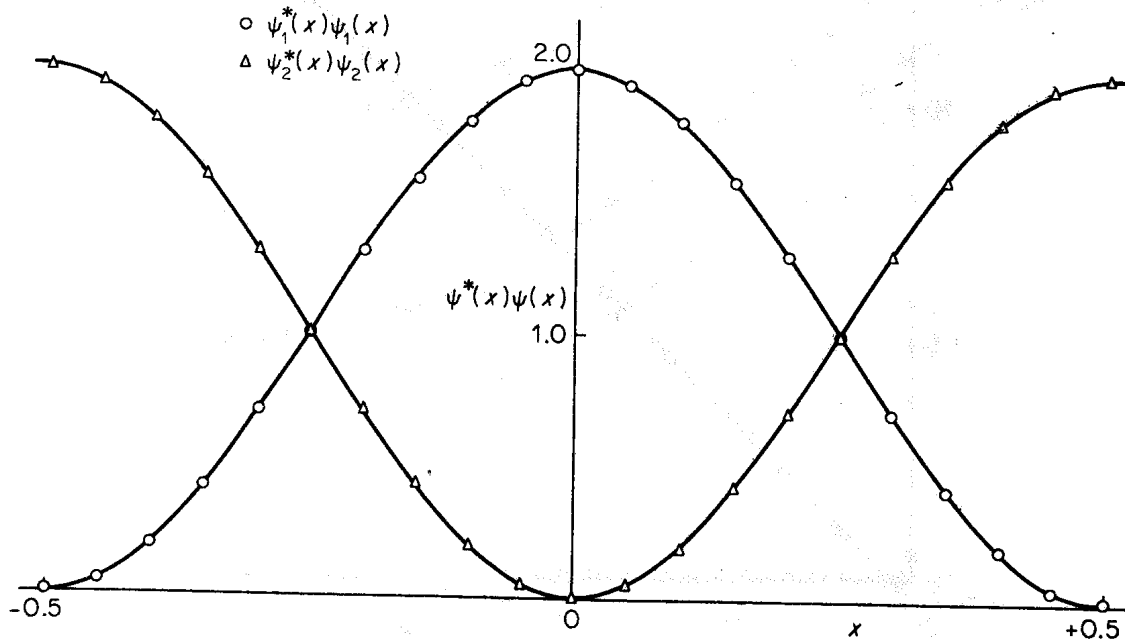

Figure 8. The results of the computer program for the probability density at $k = \pi/a$ of the first (O) and the second band ($\triangle$) for a sawtooth potential of period 1.0 with $V_0 = 1.0$. The solid curves show the predictions of the nearly-free electron approximation. Note that for the lower energy band the probability density is high where $V(x)$ is low; for the higher energy band the probability density is high where $V(x)$ is high

In Figure 8 the computed results for the probability density (the data points) are compared with the above results for the nearly-free electron approximation. The potential used was the sawtooth potential.

In view of the rather large magnitude of the Fourier components of the Coulomb potential it might be thought that the nearly-free electron approximation would be of little value in practice, and indeed, for many years, it was not clear why it gives reasonable results in many cases. The reason is that, because the 'free' electron wave functions are orthogonal to the core states, the Schrödinger equation can be transformed so that the potential can be replaced by a 'pseudopotential'[7] which is weaker than the true Coulomb potential and which has Fourier components of smaller magnitude which are rapidly convergent.

2.8 The tight-binding approximation

If $V_0 a$ is large, but not sufficiently large for the core state approximation to apply, we might expect that a good approximation to the true wave function would be a linear combination of atomic wave functions $\phi_{atom}(x)$ on each site. Bloch[4] suggested a linear combination of the form:

$$\psi_k(x) = A \sum_{n=-\infty}^{+\infty} \exp(ikna)\phi_{atom}(x-na), \qquad (59)$$

where $\phi_{atom}(x-na)$ is an atomic wave function centred on the site at na, and A is a normalizing factor.

These functions satisfy the Bloch condition $\psi_k(x) = \exp(ikx)u_k(x)$, where $u_k(x)$ is of period a. The suggested linear combination implies

$$u_k(x) = \exp(-ikx)A \sum_{n=-\infty}^{+\infty} \exp(ikna)\phi_{atom}(x-na). \qquad (60)$$

Hence

$$u_k(x+ma) = \exp\{-ik(x+ma)\}A \sum_{n=-\infty}^{+\infty} \exp(ikna)\phi_{atom}(x+ma-na)$$

$$= \exp(-ikx)A \sum_{n=-\infty}^{+\infty} \exp(ik[n-m]a)\phi_{atom}(x-[n-m]a), \qquad (61)$$

and, since the sum over n runs from $-\infty$ to $+\infty$,

$$u_k(x+ma) = \exp(-ikx)A \sum_{n=-\infty}^{+\infty} \exp(ikna)\phi_{atom}(x-na)$$

$$= u_k(x). \qquad (62)$$

Now equation (10) is

$$\langle E \rangle = \frac{\int_0^a \psi^*(x)\mathcal{H}\psi(x)\,dx}{\int_0^a \psi^*(x)\psi(x)\,dx} = \frac{N}{D}. \tag{63}$$

The denominator, using equation (60), is

$$D = \int_0^a \psi^*(x)\psi(x)\,dx$$

$$= A^*A \int_0^a \sum_{n=-\infty}^{+\infty} \exp(-ika)\phi_{atom}^*(x-na) \sum_{m=-\infty}^{+\infty} \exp(ikma)\phi_{atom}(x-ma)\,dx. \tag{64}$$

If we write $l = n - m$ equation (64) becomes

$$D = A^*A \sum_{n=-\infty}^{+\infty} \sum_{l=-\infty}^{+\infty} \exp(-kla) \int_0^a \phi_{atom}^*(x-na)\phi_{atom}(x+la-na)\,dx. \tag{65}$$

Summing over n and then integrating over the interval $0 \leqslant x \leqslant a$, i.e. over the unit cell, is equivalent to integrating over all space giving

$$D = A^*A \sum_{l=-\infty}^{+\infty} \exp(-ikla) \int_{-\infty}^{+\infty} \phi_{atom}^*(x)\phi_{atom}(x+la)\,dx. \tag{66}$$

If we write

$$S_l = \int_{-\infty}^{+\infty} \phi_{atom}^*(x)\phi_{atom}(x+la)\,dx, \tag{67}$$

equation (66) simplifies to

$$D = A^*A \sum_{l=-\infty}^{+\infty} \exp(-ikla)S_l. \tag{68}$$

(Note that S_0 is simply the norm of $\phi_{atom}(x)$.)

Major simplification occurs because, when the tight-binding approximation is appropriate, the atomic wave functions $\phi_{atom}(x)$ are highly localized, and S_l is significant only for $l = 0$ (the dominant term) and for $l = \pm 1$.

The numerator in the expression for $\langle E \rangle$ is

$$N = \int_0^a \psi^*(x) \mathcal{H} \psi(x) \, dx$$

$$= AA^* \int_0^a \sum_{n=-\infty}^{+\infty} \exp(-ikna) \phi_{\text{atom}}^*(x-na) \mathcal{H} \sum_{m=-\infty}^{+\infty}$$

$$\times \exp(ikma) \phi_{\text{atom}}(x-ma) \, dx, \quad (69)$$

and, by a similar argument, if we define

$$H_l = \int_{-\infty}^{+\infty} \phi_{\text{atom}}^*(x) \mathcal{H} \phi_{\text{atom}}(x+la) \, dx, \quad (70)$$

equation (69) becomes

$$N = A^*A \sum_{l=-\infty}^{+\infty} \exp(-ikla) H_l. \quad (71)$$

Now

$$\mathcal{H} \phi_{\text{atom}}(x+la) = \left[-\frac{d^2}{dx^2} + V(x) \right] \phi_{\text{atom}}(x+la)$$

$$= \left[-\frac{d^2}{dx^2} + U_{\text{atom}}(x+la) \right] \phi_{\text{atom}}(x+la)$$

$$+ [V(x) - U_{\text{atom}}(x+la)] \phi_{\text{atom}}(x+la), \quad (72)$$

(here $U_{\text{atom}}(x+la)$ is the atomic potential centred on the atom at $-la$). Therefore,

$$\mathcal{H} \phi_{\text{atom}}(x+la) = E_{\text{atom}} \phi_{\text{atom}}(x+la) + [V(x) - U_{\text{atom}}(x+la)] \phi_{\text{atom}}(x+la), \quad (73)$$

so that

$$H_l = \int_{-\infty}^{+\infty} \phi_{\text{atom}}^*(x) \mathcal{H} \phi_{\text{atom}}(x+la) \, dx$$

$$= E_{\text{atom}} S_l + g_l, \quad (74)$$

where

$$g_l = \int_{-\infty}^{+\infty} \phi_{\text{atom}}^*(x) [V(x) - U_{\text{atom}}(x+la)] \phi_{\text{atom}}(x+la) \, dx. \quad (75)$$

The g_l's are referred to as overlap integrals. Hence

$$\langle E \rangle = \frac{\sum\limits_{l=-\infty}^{+\infty} \exp(-ikla) \cdot (E_{\text{atom}} S_l + g_l)}{\sum\limits_{l=-\infty}^{+\infty} \exp(-ikla) S_l}$$

$$= E_{\text{atom}} + \frac{\sum\limits_{l=-\infty}^{+\infty} \exp(-ikla) g_l}{\sum\limits_{l=-\infty}^{+\infty} \exp(-ikla) S_l}, \tag{76}$$

and the only significant contributions will come from terms for small $|l|$.

Figure 9 shows some of the functions involved in the integrals which give S_l and g_l for the case of the lowest energy band with the harmonic potential. For $V_0 a \to \infty$ the only significant terms are for $l = 0$ and

$$\langle E \rangle \approx E_{\text{atom}} + \frac{g_0}{S_0}. \tag{77}$$

The first term is the core state approximation. The second term is the correction to it predicted by first-order perturbation theory.

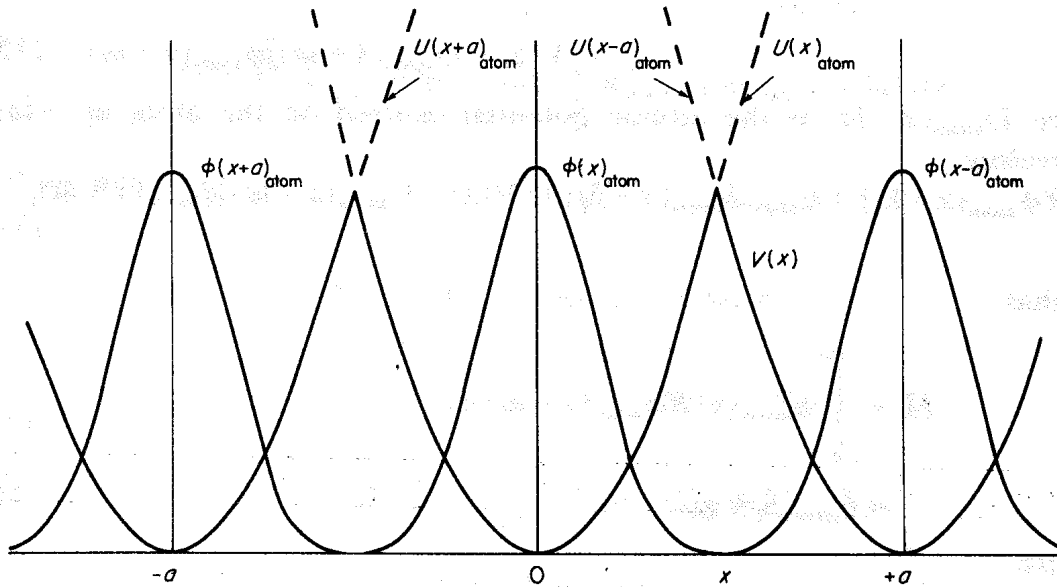For somewhat lower values of $V_0 a$ the $|l| = 1$ terms will also be significant.

Figure 9. Some of the functions involved in calculating S_l and g_l for the lowest energy band in the tight-binding approximation with the harmonic potential

Usually the term in $g_{\pm 1}$ is significant before that in $S_{\pm 1}$ and, since $g_1 = g_{-1}$,

$$\langle E \rangle \approx E_{\text{atom}} + \frac{g_0}{S_0} + \frac{g_1}{S_0} [\exp(ika) + \exp(-ika)]$$

$$= E_{\text{atom}} + \frac{g_0}{S_0} + \frac{2g_1}{S_0} \cos(ka), \tag{78}$$

and, if $\phi_{\text{atom}}(x)$ is normalized to unity,

$$\langle E \rangle = E_{\text{atom}} + g_0 + 2g_1 \cos(ka). \tag{79}$$

Thus, in the tight-binding approximation,

$$E(k=0) - E(k=\pi/a) = 4g_1 \quad \text{and} \quad E(k=\pi/2a) = E_{\text{atom}} + g_0.$$

The tight-binding approximation can be applied to the following potentials employed in the computer program:

(i) The cosine potential where, for the lowest energy band,

$$g_0 = V_0 \left(\frac{2V_0}{a^2}\right)^{\frac{1}{4}} \int_{-\infty}^{+\infty} \exp\left(-\frac{x^2\pi}{a}\sqrt{2V_0}\right)\left[1 - \cos\left(\frac{2\pi x}{a}\right) - \frac{2\pi^2 x^2}{a^2}\right] dx$$

$$= V_0\left[1 - \frac{\pi}{a\sqrt{2V_0}} - \exp\left(-\frac{\pi}{a\sqrt{2V_0}}\right)\right], \tag{80}$$

and

$$g_1 = V_0\left(\frac{2V_0}{a^2}\right)^{\frac{1}{4}} \int_{-\infty}^{+\infty} \exp\left(-\frac{x^2\pi}{a}\sqrt{\frac{V_0}{2}}\right)\left[1 - \cos\left(\frac{2\pi x}{a}\right) - \frac{2\pi^2}{a^2}(x+a)^2\right]$$

$$\times \exp\left(-\frac{[x+a]^2\pi}{a}\sqrt{\frac{V_0}{2}}\right) dx$$

$$= V_0 \exp\left(\frac{-a\pi}{2}\sqrt{\frac{V_0}{2}}\right)\left[1 - \frac{\pi^2}{2} - \frac{\pi}{a\sqrt{2V_0}} + \exp\left(-\frac{\pi}{a\sqrt{2V_0}}\right)\right]. \tag{81}$$

(ii) The harmonic potential. For the lowest band

$$g_0 \approx \frac{8}{a^2}\left(\frac{4V_0}{a^2\pi^2}\right)^{\frac{1}{4}} \int_{a/2}^{+\infty} \exp\left(-2\sqrt{V_0}\frac{x^2}{a}\right)[V_0(x-a)^2 - V_0 x^2] dx$$

$$= 4V_0\left[1 - \Phi(V_0^{\frac{1}{4}}\sqrt{a})\right] - \frac{4\sqrt{2}V_0^{\frac{3}{2}}}{\sqrt{\pi a}}\exp\left(-\sqrt{V_0}\frac{a}{2}\right), \tag{82}$$

$$g_1 \approx \frac{4}{a^2}\left(\frac{4V_0}{a^2\pi^2}\right)^{\frac{1}{4}} \int\limits_{-a/2}^{+a/2} \exp\left(-\frac{\sqrt{V_0}\,x^2}{a}\right)$$

$$\times\left[V_0 x^2 - V_0(x+a)^2\right]\exp\left(-\sqrt{V_0}\,\frac{(x+a)^2}{a}\right)dx$$

$$= 2\sqrt{2}\cdot\frac{V_0^{\frac{3}{4}}}{\sqrt{\pi a}}\exp\left(-\sqrt{V_0}\,\frac{a}{2}\right)\left[\exp(-2\sqrt{V_0}\,a)-1\right]. \tag{83}$$

For the harmonic potential the probability integral

$$\Phi(z) = \sqrt{\frac{2}{\pi}}\int\limits_{0}^{z}\exp(-t^2/2)\,dt \tag{84}$$

is required. This integral cannot be expressed in closed form. It can be approximated by a series expansion, but for the large values of z typically involved, convergence is slow and it is more convenient to use tabulated values for $\Phi(z)$.

The tight-binding approximation cannot be applied to the rectangular potential if the 'atomic' wave functions are taken to be those corresponding to an infinite potential well because in that case $g_0 = g_1 = \ldots = 0$. It can be used if the atomic states are taken as those appropriate for a finite potential well, and an approach along these lines has been presented by Wetsel[6] though the overlap integrals for the finite potential well cannot be expressed as analytic functions but involve the solution of a transcendental equation.

In Figure 10 the computed results for the variation of E with k of the lowest band (the data points) are compared with the predictions of the tightbinding approximation (the solid curves) for the harmonic potential. Agreement deteriorates as V_0 increases. In Figure 11 the circles show the computed results for $E(k = \pi/a) - E(k = 0)$ as a function of V_0 with the harmonic potential. The solid curve shows $4g_1$, i.e. the energy difference predicted by the tight-binding approximation.

2.9 The effective mass

There are situations, particularly those involving the dynamic behaviour of the electrons, when the $E - k$ relationship is not the most useful form in which to present the results of a band structure calculation. The wave function $\psi(x) = \exp(ikx)u_k(x)$ extends over all space; if we want to represent the motion of a 'localized' electron the uncertainty principle indicates that we must build up a wave-packet with a spread of k-values. The appropriate velocity is then the group velocity (V_G) which is equal to the derivative of
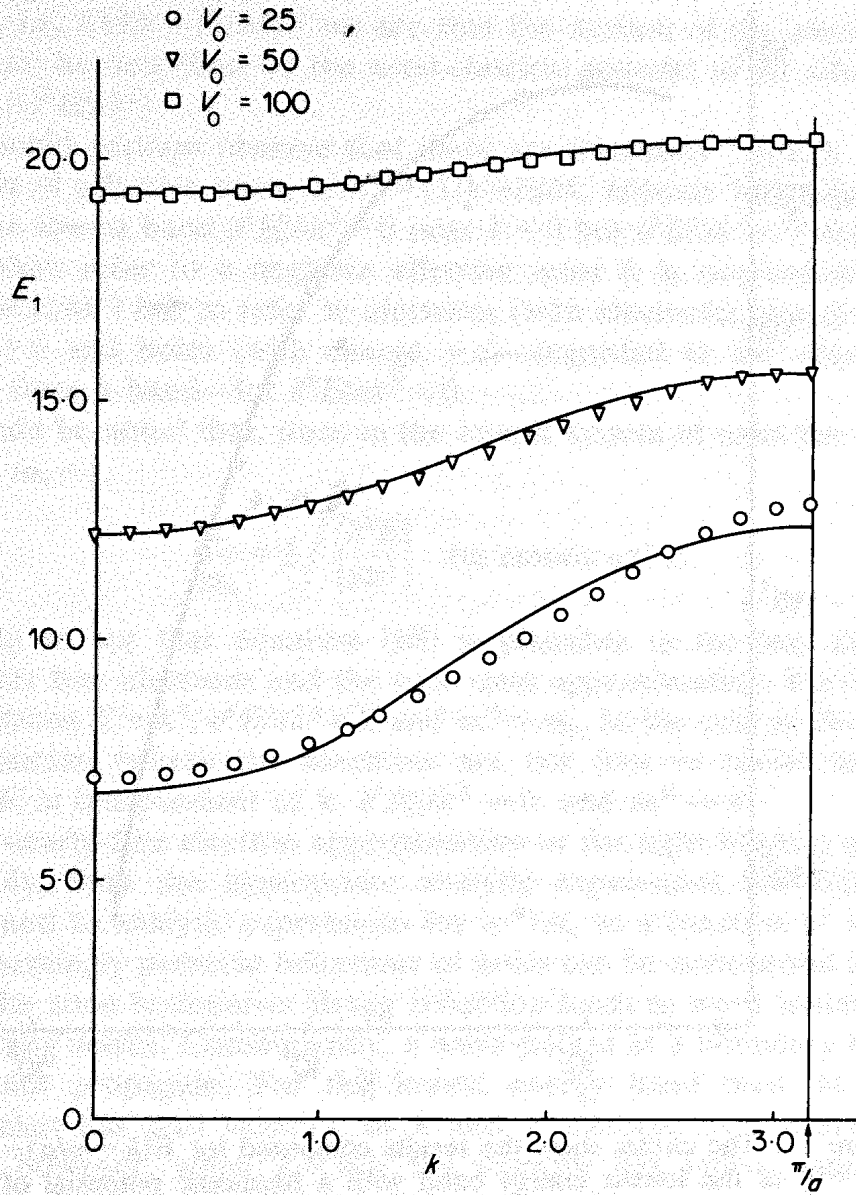
Figure 10. The results of the computer program for the lowest energy band with the harmonic potential of period 1.0 for $V_0 = 25(\bigcirc)$, $V_0 = 50(\nabla)$, and $V_0 = 100(\square)$. The solid curves show the predictions of the tight-binding approximation

the angular frequency (ω) with respect to k

$$V_G = \frac{\partial \omega}{\partial k} = \frac{\partial E}{\partial k} \tag{85}$$

$(E = \omega,$ since $\hbar = 1$ in the atomic system of units).

If a force F acts on this electron wave-packet in the $+x$-direction then

$$FV_G = \frac{\partial E}{\partial t}, \tag{86}$$
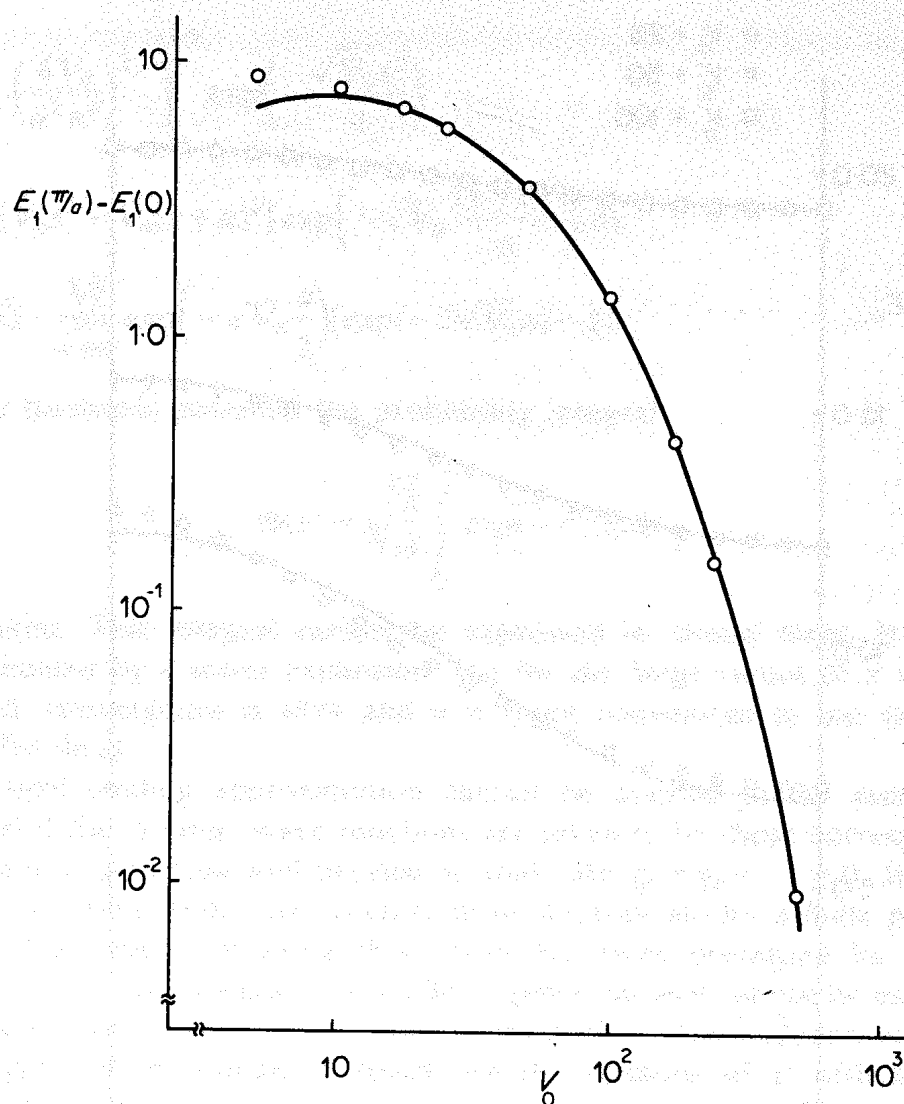
Figure 11. The circles show the results computed for $E(k = \pi/a) - E(k = 0)$ of the lowest energy band with a harmonic potential of period 1.0, as a function of V_0. The solid curve shows $4g_1$ which is the energy difference predicted by the tight-binding approximation

and

$$\frac{\partial V_G}{\partial t} = \frac{\partial}{\partial t}\left(\frac{\partial E}{\partial k}\right) = \frac{\partial}{\partial k}\left(\frac{\partial E}{\partial t}\right)$$

$$= \frac{\partial}{\partial k}(FV_G) = \frac{\partial}{\partial k}\left(F\frac{\partial E}{\partial k}\right)$$

$$= F\frac{\partial^2 E}{\partial k^2}. \tag{87}$$

Comparing this result with Newton's second law of motion for a particle of

mass M, i.e. $\partial V/\partial t = (1/M)F$ we see that the motion of the electron wave-packet can be described by the semi-classical concept of an effective mass $(m^*) = 1/(\partial^2 E/\partial k^2)$.

We should perhaps observe that there are situations[8,9] where a different definition of effective mass, $1/m^* = (1/k)\partial E/\partial k$, appears to be appropriate.

For the lowest band $\partial^2 E/\partial k^2 > 0$ near $k = 0$ but $\partial^2 E/\partial k^2 < 0$ near $k = \pi/a$. Rather than refer to a negative effective mass it is conventional to take $m^* = 1/|\partial^2 E/\partial k^2|$ but to refer to electrons (with electronic charge $-e$) when $\partial^2 E/\partial k^2 > 0$ and holes (with charge $+e$)—regarded as the *absence* of an electron from a band—for $\partial^2 E/\partial k^2 < 0$.

It should be noted that, since in the atomic system of units the mass of an electron $m_e = \frac{1}{2}$,

$$\frac{m^*}{m_e} = 2 \bigg/ \left|\frac{\partial^2 E}{\partial k^2}\right| \quad \text{(in atomic units).} \tag{88}$$

It is easy to see that equation (88) is plausible in the two extremes of completely free electrons and the core state approximation. For completely free electrons $E = k^2$, $\partial^2 E/\partial k^2 = 2$ and $m^* = m_e$. In the case of the core state approximation (where the electrons are not free to travel through the crystal) E is independent of k, $\partial^2 E/\partial k^2 \to 0$, and $m^* \to \infty$.

If the nearly-free electron approximation or the tight-binding approximation apply, then the appropriate analytic expressions for $E(k)$ can be transformed to analytic expressions for m^*/m_e as a function of k.

The seemingly perverse behaviour of holes can be understood if we recall that at the zone boundaries Bragg reflection leads to wave functions which are standing waves. Consequently, a wave-packet at a boundary has $V_G = 0$ and cannot propagate. For the lowest energy band then, at $k = 0$ the wave-packet has zero velocity; as k and E increase its velocity increases initially, however, when $k = \pi/a$ the velocity has fallen again to zero. Consequently, there are regions of the energy bands approaching the zone boundaries where an *increase* in energy leads to a *decrease* in velocity—the acceleration is in the opposite direction to the force. The concept of holes is used to describe this unexpected behaviour.

Having found E at $k = 0$, $\pi/20a$, $\pi/10a$, ..., π/a the program estimates $\partial^2 E/\partial k^2$ at these k-values from the results for $E_{k-\Delta k}$, E_k, and $E_{k+\Delta k}$. By Taylor's series:

$$E_{k+\Delta k} = E_k + \frac{\Delta k}{1!}\frac{\partial E}{\partial k} - \frac{\Delta k^2}{2!}\frac{\partial^2 E}{\partial k^2} + \cdots. \tag{89}$$

Hence

$$\left(\frac{\partial^2 E}{\partial k^2}\right)_k \approx \frac{1}{\Delta k^2}[E_{k+\Delta k} + E_{k-\Delta k} - 2E_k]. \tag{90}$$

The program displays the results for m^*/m_e as a function of k, printing a letter E (electron) when $\partial^2 E/\partial k^2 > 0$ and a letter H (hole) when $\partial^2 E/\partial k^2 < 0$.

2.10 The probability density

The variation of E with k (or related variables) is usually the most important result of a band structure calculation. There are, however, situations when the actual wave functions or related quantities are of interest. In particular the total electron probability density, which can be investigated by X-ray and neutron diffraction techniques, according to equation (3) involves the product $u_k^*(x)u_k(x)$. Now

$$u_k(x) = \sum_{l=-N}^{+N} c_l \exp\left(\frac{i2\pi l x}{a}\right),\tag{91}$$

and for systems with an inversion centre, the Hamiltonian matrix is real. Consequently the c_l's are real, and

$$u_k^*(x) = \sum_{m=-N}^{+N} c_m \exp\left(-\frac{i2\pi m x}{a}\right).\tag{92}$$

Hence

$$
\begin{aligned}
u_k^*(x)u_k(x) &= \sum_{m=-N}^{+N} c_m \exp\left(-\frac{i2\pi m x}{a}\right) \sum_{l=-N}^{+N} c_l \exp\left(\frac{i2\pi l x}{a}\right) \\
&= \sum_{m=-N}^{+N} \sum_{l=-N}^{+N} c_m c_l \exp\left(i2\pi[l-m]\frac{x}{a}\right) \\
&= \sum_{m=-N}^{+N} \sum_{l=-N}^{+N} c_m c_l \cos\left(2\pi[l-m]\frac{x}{a}\right) \\
&= 1 + 2 \sum_{m=-N}^{+N} \sum_{l=m+1}^{+N} c_m c_l \cos\left(2\pi[l-m]\frac{x}{a}\right),
\end{aligned}\tag{93}
$$

since $\sum_{m=-N}^{+N} c_m^2 = 1$ and $u_k^*(x)u_k(x)$ is real.

The computer program finds the probability densities in the range $-a/2 < x < a/2$ for a value of k specified by the user. The results can be compared with the predictions of the core state approximation or the nearly-free electron approximation when they are appropriate.

As is generally the case when the variational method is employed, the results for the probability density can be expected to be less accurate than the results for the energy.

3. THE COMPUTER PROGRAM

The program allows the user to choose the potential from the set of even periodic functions described in section 2.5. The first section prints questions

about the potential. The program as written is for use on an interactive system. This section would need to be modified for use in batch mode. The user's responses define the potential function by setting the integer variable NPOT and the value of constants, such as the period and the maximum value of the potential.

The subroutine FRANCS(NTERMS, NDATA, DC, A) is then called to find the coefficients of the cosine terms in the Fourier series. The first parameter NTERMS ($=33$) is the number of coefficients required. NDATA ($=$ NPTS) is used only when the interpolated potential is employed. For that particular case FRANCS( ) employs trapezoidal integration and NDATA specifies the number of subdivisions required. The fourth parameter DC is the constant term in the Fourier series for $V(x)$, i.e. $d_0/2$. The fifth parameter is the array A( ) which is set by FRANCS( ) to the Fourier coefficients; $A(1) = d_1$, $A(2) = d_2, \ldots, (A33) = d_{33}$. In the case of all except the interpolated potential the Fourier coefficients are determined analytically.

Next $K(=k)$ is set. It is increased in 20 steps from 0 to π/a. Because the true matrix for the Hamiltonian is of infinite dimension in practice it has to be truncated, which introduces some error into the results. In an attempt to maintain this error less than ~ 1 per cent the dimension of the Hamiltonian (NAR) is set initially to either 10 or 11. The energies are then determined by the subroutine ENERGY( ) and NAR increased by 2. ENERGY( ) is called again and if the fractional changes in the results for the energy are less than 3×10^{-3} then they are printed out. If one or more of the results has changed by more than 3×10^{-3}, NAR is increased by a further 8 and ENERGY( ) called again.

This process is continued till NAR is 32 or 33. At this point the computing time taken becomes significant, so rather than increasing NAR further, the results are printed out with an accuracy warning. If higher accuracy were to be required the program could be modified by increasing the upper limit on NAR.

The subroutine ENERGY(K, E, EV, ND, N, DC, A, H, W, BOOL) is used to find the energy eigenvalues and also (if BOOL is set.FALSE.) the eigenvectors.

The parameters set on entry are: $K(=k)$, ND – the first dimension of H( ) (the Hamiltonian) as specified in ENERGY( ), N is the order of H( ), DC and A( ) are the Fourier coefficients described above and BOOL is a logical variable. If BOOL is set .TRUE. the NAG[10] library routine F02AAF()—which calculates eigenvalues—is called. If BOOL is set .FALSE. the NAG routine F02ABF( )—which calculates eigenvalues and eigenvectors—is called.

ENERGY( ) sets up the Hamiltonian matrix H( ). The input variables common to F02AAF( ) and F02ABF( ) are H( ), ND, N (as described above), and IFAIL which specifies what will happen if a failure occurs

during a call to these routines. Both F02AAF and F02ABF require H( )
to be real and symmetric. The array W( ) is used by the NAG routines as
working space. On exit from F02AAF or F02ABF E( ) contains the
eigenvalues *in ascending order*. On exit from F02ABF the array EV( )
contains the *normalized* eigenvectors in columns corresponding to the
eigenvalues. By calling ENERGY( ) for varying values of k the program
calculates and prints out results for the E–k diagram, showing the three
lowest energy bands.

   The user has the option of plotting these results on the line printer. The
plot is done by the subroutine GRAPH(Y, NP, NG, X). Y( ) contains the
energy values and X( ) the corresponding k-values. If a more sophisticated
graph-plotting routine were to be available to the reader GRAPH( ) could
be replaced.

   The user may also calculate the approximate effective mass as a function
of k and the probability density function as a function of x (x being
increased in 20 steps from $-a/2$ to $+a/2$), for a chosen value of k. For the
probability density function calculation ENERGY( ) is called with
BOOL = .FALSE. so that F02ABF( ) is now called. The potential is also
found as a function of x by the function V(Y) and printed out with the
corresponding probability density.

   The calculations of the probability density and the effective mass will be
less accurate than the eigenvalue calculations, especially the effective mass
results which are only intended to give a qualitative picture of the variation
of m^*/m_e with k. In both cases there is the option of plotting the results
graphically.

   Finally the user has the option of either stopping or of changing the
potential and initiating a further set of calculations.

   Because of the necessary truncation of the Hamiltonian matrix there is
always some error. It is found that significant errors (accompanied by a
warning message) generally occur in the extreme core-state limit. This is
only to be expected because the very large potential values involved
generate large—and non-negligible—Fourier terms, even for the higher
terms in the series. For example, the jth coefficient for the harmonic
potential is

$$d_j = \frac{2 V_0 a \cos(j\pi)}{(j\pi)^2}$$

The magnitude of these Fourier terms decreases as j increases but increases
with increasing $V_0 a$.

3.1 A typical session

If the rectangular potential is used with:

$$V_0 = 5.0 \qquad\qquad \text{(in Rydbergs)}$$

Period $(a) = 1.5$,   (in Bohr radii)

Width of rectangle $(b) = 0.5$ (in Bohr radii)

and if computation of the effective mass and the probability density are requested then the results of the computer program are:

```
PROGRAM TO CALCULATE FIRST THREE ENERGY LEVELS OF
AN ELECTRON SUBJECT TO A GIVEN PERIODIC POTENTIAL.
ALL INPUT AND OUTPUT IS IN ATOMIC UNITS
I.E. THE UNIT OF DISTANCE IS ONE BOHR RADIUS
THE UNIT OF ENERGY IS ONE RYDBERG

WHAT SORT OF POTENTIAL DO YOU WANT
TYPE 1 FOR RECTANGULAR POTENTIAL
TYPE 2 FOR SAWTOOTH POTENTIAL
TYPE 3 FOR COSINE POTENTIAL
TYPE 4 FOR HARMONIC POTENTIAL
TYPE 5 FOR INTERPOLATED POTENTIAL
1
RECTANGULAR POTENTIAL
INPUT HEIGHT OF RECTANGLE AS REAL NUMBER
5.0
INPUT WIDTH OF RECTANGLE AS REAL NUMBER
0.5
INPUT PERIOD AS REAL NUMBER
1.5


      PERIOD        1.5


      K        E1        E2        E3
   0.0000    1.4499    18.4804   20.0641
   0.1047    1.4603    18.1049   20.4621
   0.2094    1.4917    17.4000   21.2342
   0.3142    1.5440    16.6373   22.1089
   0.4189    1.6171    15.8717   23.0315
   0.5236    1.7109    15.1179   23.9872
   0.6283    1.8253    14.3814   24.9709
   0.7330    1.9600    13.6649   25.9800
   0.8378    2.1147    12.9698   27.0133
   0.9425    2.2890    12.2974   28.0700
   1.0472    2.4824    11.6486   29.1497
   1.1519    2.6940    11.0245   30.2523
   1.2566    2.9226    10.4265   31.3775
   1.3614    3.1666     9.8564   32.5252
   1.4761    3.4233     9.3169   33.6951
   1.5708    3.6884     8.8125   34.8874
   1.6755    3.9548     8.3501   36.1018
   1.7802    4.2107     7.9419   37.3383
   1.8850    4.4355     7.6082   38.5968
   1.9897    4.5970     7.3814   39.8768
   2.0944    4.6571     7.2995   41.1096


DO YOU WANT TO PLOT THESE RESULTS
 TYPE YES OR NO
YES
```
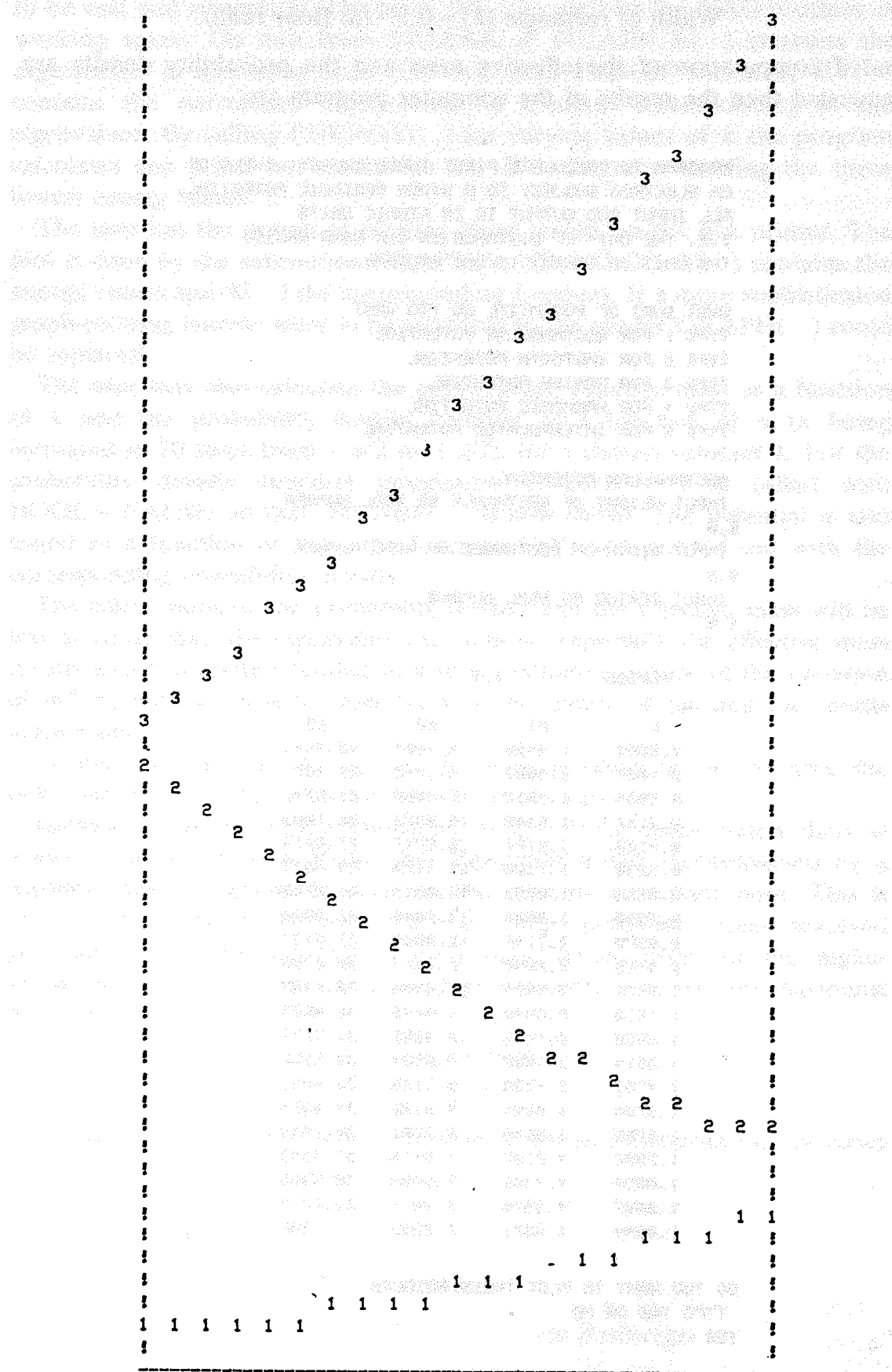
E-K DIAGRAM SHOWING FIRST THREE ENERGY LEVELS

E-K DIAGRAM SHOWING FIRST THREE ENERGY LEVELS

```
DO YOU WANT TO CALCULATE THE EFFECTIVE MASS
 TYPE YES OR NO
YES


THE MASS OF A FREE ELECTRON IS 1.0


         K          M1          M2          M3
      0.0000     1.05 E      0.03 H      0.03 E
      0.1047     1.05 E      0.07 H      0.06 E
      0.2094     1.05 E      0.38 H      0.21 E
      0.3142     1.05 E      7.40 H      0.46 E
      0.4189     1.06 E      1.86 E      0.66 E
      0.5236     1.07 E      1.27 E      0.79 E
      0.6283     1.08 E      1.10 E      0.86 E
      0.7330     1.10 E      1.02 E      0.91 E
      0.8378     1.12 E      0.97 E      0.93 E
      0.9425     1.15 E      0.93 E      0.96 E
      1.0472     1.20 E      0.89 E      0.96 E
      1.1519     1.28 E      0.84 E      0.97 E
      1.2566     1.43 E      0.79 E      0.98 E
      1.3614     1.73 E      0.71 E      0.98 E
      1.4661     2.60 E      0.63 E      0.99 E
      1.5708    15.80 E      0.52 E      0.99 E
      1.6755     2.07 H      0.41 E      0.99 E
      1.7802     0.71 H      0.29 E      1.00 E
      1.8850     0.35 H      0.21 E      1.02 E
      1.9897     0.22 H      0.15 E      0.47 H
      2.0944     0.18 H      0.13 E      0.01 H


DO YOU WANT TO PLOT THESE RESULTS
 TYPE YES OR NO
NO
```

DO YOU WANT TO CALCULATE THE PROBABILITY DENSITY
FUNCTIONS FOR THE FIRST THREE ENERGY STATES
TYPE YES OR NO
YES
 INPUT A VALUE OF K AS A REAL NUMBER
2.0944

X	PD1	PD2	PD3	V
-0.7500	-0.0000	1.7479	-0.0000	5.0000
-0.6750	0.0410	1.7247	0.3807	5.0000
-0.6000	0.1640	1.6579	1.2313	5.0000
-0.5250	0.3712	1.5536	1.9127	5.0000
-0.4500	0.6541	1.3909	1.8729	0.0000
-0.3750	0.9788	1.1409	1.0989	0.0000
-0.3000	1.3072	0.8310	0.2388	0.0000
-0.2250	1.6075	0.5166	0.0327	0.0000
-0.1500	1.8471	0.2462	0.6556	0.0000
-0.0750	2.0014	0.0641	1.5750	0.0000
0.0000	2.0552	-0.0000	2.0028	0.0000
0.0750	2.0014	0.0641	1.5750	0.0000
0.1500	1.8471	0.2462	0.6556	0.0000
0.2250	1.6075	0.5166	0.0327	0.0000
0.3000	1.3072	0.8310	0.2388	0.0000
0.3750	0.9788	1.1409	1.0989	0.0000
0.4500	0.6541	1.3909	1.8729	0.0000
0.5250	0.3712	1.5536	1.9127	5.0000
0.6000	0.1640	1.6579	1.2313	5.0000
0.6750	0.0410	1.7247	0.3807	5.0000
0.7500	-0.0000	1.7479	-0.0000	5.0000

DO YOU WANT TO PLOT THESE RESULTS
 TYPE YES OR NO
YES